Microbial Cysteine Degradation Drives Cryptic Sulfide Redox Chemistry in the Gut

Sarah Wolfson
Albert Einstein College of Medicine https://orcid.org/0000-0001-9774-0977
Reese Hitchings
Albert Einstein College of Medicine
Karina Peregrina
Albert Einstein College of Medicine
Ziv Cohen
Albert Einstein College of Medicine
Saad Khan
Albert Einstein College of Medicine
Tugba Yilmaz
Northeastern University
Marcel Malena
Albert Einstein College of Medicine
Edgar Goluch
Northeastern University
Leonard Augenlicht
Albert Einstein College of Medicine
Libusha Kelly (libusha.kelly@einsteinmed.org)
Albert Einstein College of Medicine

Research Article

Keywords: hydrogen sulfide, gut chemical landscape, cysteine metabolism

Posted Date: October 1st, 2021

DOI: https://doi.org/10.21203/rs.3.rs-909548/v1

Version of Record: A version of this preprint was published at Nature Metabolism on October 20th, 2022. See the published version at https://doi.org/10.1038/s42255-022-00656-z.

Abstract

Although microbial biochemistry shapes a dynamic environment in the gut, how bacterial metabolites such as hydrogen sulfide (H_2S) mechanistically alter the gut chemical landscape is poorly understood. Here we show for the first time that H_2S generated during cysteine metabolism drives the reduction of azo (R-N=N-R') xenobiotics in bacterial cultures, human fecal microbial communities, and *in vivo* mouse models. Thus, chemical-chemical interactions, derived from microbial community metabolism, are a key missing feature shaping xenobiotic metabolism in the gut. Changing dietary levels of the H_2S xenobiotic redox partner Red 40 transiently decreases mouse fecal sulfide, confirming that a xenobiotic can attenuate sulfide concentration *in vivo*. Cryptic H_2S redox thus modulates sulfur homeostasis in the gut and the fate of xenobiotics to which humans are regularly exposed.

Main Text

In microbial ecosystems, functional chemistry is dictated by microbial metabolism. Our gut microbiota produce millimolar quantities of hydrogen sulfide (H_2S/HS^-)[1], a highly redox active molecule. Sulfur is an essential element for all life and under physiological conditions in the human gut is found between the -2 and +6 redox states[2]. Biogenic hydrogen sulfide is a Janus-faced molecule in the gut[3]; while it is toxic to colonocytes[1,4] and mediates antibiotic resistance in bacterial pathogens[5], hydrogen sulfide also promotes mucosal integrity[6] and can be neuroprotective[7]. Here we show for the first time that hydrogen sulfide abiotically transfers electrons to dietary and xenobiotic redox partners in the gut, alleviating accumulation of H_2S, modulating xenobiotic metabolism, and shaping the gut chemical landscape.

To investigate hydrogen sulfide redox chemistry with common xenobiotics in the gut, we used azo (R-N=N-R') chemicals as model potential redox partners. Azo compounds are structurally diverse and common in Western foods and drugs[8]. Critically, physiological effects of many azo chemicals are dictated by reduction of the azo bond. For example, the prevalent azo food dye FD&C Red No. 40 (Red 40) is a potent inhibitor of the human intestinal transporter OATP2B1, while azoreduction of this dye by the gut microbiome rescues inhibition[9]. Azoreduction, however, does not always benefit the host. Cleavage of the azo bond in Red 40 was also recently found to induce colitis in mice overexpressing IL-23[10].

Human luminal H_2S concentrations range from 0.5-3 mM[11]. Consumption of animal protein correlates with higher luminal H_2S due to high levels of cysteine[1]. The mammalian lumen also contains endogenous sulfur sources such as glycans (e.g. mucins) in the mucosa[12], which can be microbially degraded to H_2S. In the human gut, the mechanism of azoreduction is currently assumed to proceed

enzymatically through the activity of microbial azoreductases[13]. However, outside of the host environment, in wastewater treatment of industrial azo dyes, azoreduction has also been shown to occur via abiotic chemical reduction mediated by the H_2S released as a byproduct of sulfate respiration by sulfate reducing bacteria. In abiotic azoreduction, two molecules of H_2S transfer four electrons to the azo bond directly or via a redox mediator, resulting in azo fission and oxidation of H_2S to zero valent sulfur (S^0)[14]. Given the universal presence of H_2S in the human gut, we hypothesized that the same chemical fission of azo compounds via sulfide redox could occur.

It was first determined whether H_2S can reduce azo food dyes and drugs[8] in the absence of biological activity. In sterile anoxic buffer, H_2S transfers its electrons to the azo bond, resulting in bond cleavage and two aminated daughter compounds (Fig. 1a). Five structurally diverse azo compounds representing anti-inflammatory azo-prodrugs as well as food and industrial dyes, all relevant to human exposures, were added to sterile, anoxic buffer containing a physiological concentration (3 mM)[1,11] of hydrogen sulfide. Experiments were carried out in phosphate buffer, with or without flavin mononucleotide (FMN), because redox mediators like FMN and quinone compounds increase the rate of azoreduction by bacteria[15,16]. The reaction proceeded for 6 hours and then was halted by precipitating sulfide with excess zinc acetate. Expected azoreduced aromatic amine products, confirmed by LCMS analysis, were generated at a rate reciprocal to the decrease in the azo parent compound (Fig. 1b, Supplementary Fig. 1). Furthermore, direct electron transfer from sulfide to the azo-prodrugs balsalazide (BSZ) and sulfasalazine (SSZ) was observed. Azoreduction of common food dyes Red 40 and Yellow 6, and the industrial dye Congo Red, were dependent upon FMN, indicating that FMN is an electron shuttle for reduction of these compounds.

To determine the relationship between the redox potential and propensity for H_2S reduction, cyclic voltammetry was used to obtain the redox potentials of the azo bonds in compounds from Fig. 1b. We observed a threshold of -0.55mV below which FMN was required for azoreduction (Fig. 1c). Characterizing abiotic electron transfer from H_2S to the azo bond in foods and drugs informs the mechanism of potential sulfide redox chemistry in the gut.

In the gut environment hydrogen sulfide is produced principally by bacterial degradation of thiols, particularly the amino acid cysteine[11]. To directly interrogate the propensity for H_2S azoreduction in the background of expected enzymatic azoreduction, H_2S azoreduction from cysteine degradation was determined in a bacterium containing known azoreductases. *E. coli* K-12 W3100 was incubated under strict anoxic conditions with Red 40 at 0.25 mM, 0.5 mM, and 3.0 mM, with or without the addition of cysteine (Fig. 2a). Cysteine contains one thiol moiety and during dissimilatory metabolism releases

stoichiometric H_2S[17]. Given the 2:1 ratio of H_2S to azo required for azoreduction, 2 mM cysteine theoretically supplies sufficient sulfur for the lower two Red 40 conditions, while the 3 mM Red 40 condition contains excess azo relative to supplemented sulfur. Controls included unamended LB media to determine the extent of enzymatic *E. coli* azoreduction and sulfide production in a standard medium under anoxic conditions, and serine supplemented media which provides an analogue amino acid missing the thiol moiety. Only cultures amended with cysteine eliminated Red 40 (Fig. 2a, top panel). Red 40 was completely azoreduced in 0.25 and 0.5 mM cultures within 7 and 9.5 hours, respectively. In the initial 5 hours of incubation, sulfide generation was equal among all cysteine conditions. During this time H_2S accumulated to ~ 2 mM, indicating near complete dissimilatory cysteine degradation. No Red 40 azo cleavage was observed by *E. coli* in anoxic LB. Cultures supplemented with serine behaved identically to LB media controls, indicating that any benefit from additional amino acid influenced neither azoreduction nor H_2S generation. The 3 mM cultures lost 0.82 mM Red 40 during the experimental window; this incomplete loss further indicates the lack of azoreductase activity under these conditions. To quantify the H_2S that donated its electrons to Red 40, H_2S in each Red 40 condition was compared to that in the Red 40-free control, which served as a reference for the maximum H_2S potential (Fig. 2b). After the initial 5 hours of incubation during which H_2S was equal among all cysteine conditions, Red 40 loss began and sulfide decreased in parallel with Red 40 loss until Red 40 was completely azoreduced. Only after complete Red 40 loss did sulfide concentrations again increase. Thus, the observed H_2S concentration as a function of time was not the absolute amount generated during cysteine degradation, but rather the net of H_2S generation and H_2S oxidation via Red 40. In the gut, where many compounds may serve as electron acceptors from H_2S, measured H_2S concentrations are a net value of these competing reactions.

The absence of Red 40 azoreduction in control *E. coli* cultures indicated that enzymatic activity is not responsible for Red 40 loss under these conditions. To confirm this, enzymatic activity was eliminated while preserving all metabolites of cysteine, including volatile H_2S, by heat inactivation of overnight cultures in sealed vials (121°C, 25 minutes). H_2S accumulated to ~2 mM, indicating complete cysteine degradation. After a 1-hour re-equilibration at 37°C, Red 40 was spiked in at the three experimental concentrations. The results following heat inactivation mirrored the live *E. coli* incubations – Red 40 loss was observed only in the spent medium of *E. coli* grown with supplemented cysteine (Fig. 2c). No azoreduction was detected in control cultures. Thus, a metabolite of cysteine degradation was responsible for abiotic azoreduction in the absence of enzymatic and other biological activity.

Sulfide was measured in parallel with Red 40 to elucidate the mechanism of sulfide attenuation observed in *E. coli* exposed to Red 40. In the absence of Red 40, sulfide concentrations were constant (Fig. 2c). The addition of Red 40 stimulated loss of sulfide proportional to the concentration of Red 40. Sulfide concentrations decreased in an approximate 2:1 stoichiometric ratio to the concentration of reduced Red

40 (Fig. 2d). In live biological systems sulfide can be simultaneously generated and oxidized, obscuring direct observation of the redox reaction. The stoichiometric, concomitant decrease of sulfide and Red40 seen in the absence of microbial activity illustrates the cryptic nature of sulfide redox chemistry.

The prevalence of azo-compounds in Western diets as food dyes is of particular concern because the compounds themselves as well as their metabolites can have physiological effects[9]. Given cysteine's abundance in dietary protein, we investigated the relative change in sulfide accumulation and azoreduction induced by nutritional and endogenous sulfur sources. A healthy human microbiome was recapitulated from a human fecal sample cultured in anoxic defined media, with subcultures supplemented with different physiological sulfur (i.e. thiol) sources. These included the amino acid cysteine, bovine serum albumin (BSA) as an analog of dietary animal protein, and the highly thiolated endogenous glycoprotein mucin. Thiol-supplemented anaerobic cultures produced more sulfide (Fig. 3a) and reduced Red 40 at a higher rate (Fig. 3b) than thiol-free counterparts. The rate of azoreduction was inversely proportional to the maximum amount of H_2S generated in each condition, with significant differences in the rates of Red 40 reduction among groups (one-way ANOVA ($F(6, 14) = 8.828$, $p < 0.001$). Notably, H_2S did not begin to accumulate above background in any of the cultures until the azo substrate was exhausted at approximately 4 hours (Fig. 3a), similar to the pattern observed in live *E. coli* cultures (Fig. 2a). Thus, we observe cryptic sulfide redox chemistry dictating the concentration of sulfide in real time, providing direct evidence that sulfide azoreduction in the human gut is distinct from enzymatic azoreduction and is a fundamental contributor to total azoreduction by human gut microbiota.

Bioinformatic analysis of sulfide generating enzymes in the gut microbiota was consistent with this direct assessment of hydrogen sulfide production by the human microbiome and highlights the importance of abiotic H_2S redox in human gut physiology. Sequences of nine genes encoding enzymes with sulfidogenic cysteine degradation activity[5,17–19] were searched against the Metaquery database[20]. The proteins CBS (K01697), CSE (K01758), CysK (K01738), CysM (K12339), CyuA (COG3681), MalY (K14155), MetC (K01760), SseA (K01011) and TnaA (K01667) were analyzed for mean copy number per cell in 2,271 annotated metagenomic samples. CysK and MalY are both present at >1 copy per cell (Fig. 3c). The lower abundances of the other seven proteins suggest that subsets of the human gut microbiome make different contributions to sulfide production. We therefore sought to identify these enzymes in common human gut microbes with completely sequenced genomes to assess the distribution of sulfidogenic cysteine degradation in the human gut (Fig 3d, Supplementary Table 1). We found that multiple sulfidogenic cysteine degrading enzymes are present in the genomes of diverse, abundant, gut microbes. Of note are 7 cysteine degrading enzymes in both *Bacteroides ovatus* and *Enterococcus faecalis,* microbes recently implicated in inducing colitis via Red 40 azoreduction[10]. In conjunction with the *E. coli* and fecal microcosm data, cysteine degradation to H_2S lends mechanistic support by which *B. ovatus* and *E. faecalis* can azoreduce Red 40 and Yellow 6 to the colitis-inducing product 5-amino-6-

hydroxynaphthalene-2-sulfonic acid. Together, these results support the conclusion that H_2S biogenesis through cysteine metabolism is a “core” function of the human gut microbiome, regardless of individual community composition (Fig. 3c, d). The pervasiveness of the 9 sulfidogenic cysteine degrading enzymes among diverse human microbiomes shifts focus away from individual microbes as reducers of Red 40 and towards Red 40 reduction as a community-level function.

These results indicate that many common gut bacteria can release H_2S from cysteine and thus modulate redox chemistry in the gut environment. We therefore directly tested the potential for diet to influence H_2S biogenesis and H_2S-azo redox. Healthy mice with intact, uncontrolled microbiomes were fed purified diets differing in cysteine and Red 40 concentrations. The diets contained a standard concentration of cysteine (4 g/kg)[21], double that level (8 g/kg), or with cysteine eliminated from the diet (0 g/kg) (Supplementary Table 2) (3 separate cohorts, N=30, 10/diet). Methionine, an essential sulfur amino acid, was present at 1.6 g/kg in all three diets[22]. After two weeks, mice with uncontrolled microbiomes fed 0 g/kg cysteine produced significantly less fecal sulfide than those consuming a standard cysteine diet (Fig. 4a; Wilcoxon rank-sum test). Mice consuming 8 g/kg, did not differ in fecal sulfide compared to the standard diet (Supplementary Fig. 2). Tuning hydrogen sulfide via cysteine changes was therefore achieved through decreasing cysteine, but not increasing cysteine. We next addressed if hydrogen sulfide in mouse guts was decreased by administration of azo compounds as we observed in *E. coli* and human fecal microcosms. A controlled diet with standard cysteine levels (4 g/kg) was fed to two cohorts of mice, and after two weeks Red 40 was added to the diet of one cohort (N=20, 10 each ± Red 40). There was a transient decrease in hydrogen sulfide post-Red 40 administration (Fig. 4b), confirming that an azo-containing xenobiotic can attenuate sulfide concentration in animal guts. Hydrogen sulfide electron transfer to the azo redox partner Red 40 therefore alters fecal H_2S concentrations *in vivo*. Cryptic H_2S redox is thus responsible for gut chemistry previously thought to be solely enzymatic. Sulfide concentrations returned to pre-Red 40 levels after 4 days, suggesting the existence of complex sulfur electron transfer occurring between the gut chemical landscape, microbiota, and host on longer time scales.

Here, we establish gut sulfur redox transformation *in vivo*, initiating from the thiol group of cysteine that is liberated as H_2S and then oxidized to zero valent sulfur (Fig. 4c). Altering concentrations of the reactants in diet, i. e. cysteine as a sulfide source or an azo compound as an oxidizing agent, alters metabolite concentrations in the gut environment. These data establish a microbiome-mediated role in the abiotic redox pairing of sulfide with dietary and pharmaceutical compounds and may inform human physiological effects of gut redox state and sulfur homeostasis[3,23,24].

Hydrogen sulfide is a driver of redox chemistry, both altered by, and in turn altering, dietary and pharmaceutical compounds. Therefore, our characterization of microbially produced hydrogen sulfide as a modifier of gut redox is a novel mechanism by which gut microbiota shape their environment, revealing dynamic chemical-chemical interactions, derived from community microbiota metabolism, as essential in structuring the human gastrointestinal ecosystem. Hydrogen sulfide plays a role in cardiac homeostasis[25,26], neuroprotection in the brain[7], inflammatory bowel disease and colorectal cancer[6] and microbial defense against pathogens[24], highlighting the potential far-reaching significance of microbial sulfide production and cryptic sulfur redox in the human body.

References

1. Magee, E. A., Richardson, C. J., Hughes, R. & Cummings, J. H. Contribution of dietary protein to sulfide production in the large intestine: an in vitro and a controlled feeding study in humans. *Am J Clin Nutr* <background-color:#FFCC66;bvertical-align:super;>72</background-color:#FFCC66;bvertical-align:super;>, 1488–1494 (2000).
2. Barton, L. L., Ritz, N. L., Fauque, G. D. & Lin, H. C. Sulfur Cycling and the Intestinal Microbiome. *Dig Dis Sci* <background-color:#FFCC66;bvertical-align:super;>62</background-color:#FFCC66;bvertical-align:super;>, 2241–2257 (2017).
3. Hanson, B. T. *et al.* Sulfoquinovose is a select nutrient of prominent bacteria and a source of hydrogen sulfide in the human gut. *ISME J* 1–13 (2021) doi:10.1038/s41396-021-00968-0.
4. Guidotti, T. L. Hydrogen Sulfide: Advances in Understanding Human Toxicity. *Int J Toxicol* <background-color:#FFCC66;bvertical-align:super;>29</background-color:#FFCC66;bvertical-align:super;>, 569–581 (2010).
5. Shatalin, K., Shatalina, E., Mironov, A. & Nudler, E. H2S: A Universal Defense Against Antibiotics in Bacteria. *Science* <background-color:#FFCC66;bvertical-align:super;>334</background-color:#FFCC66;bvertical-align:super;>, 986–990 (2011).
6. Motta, J.-P. *et al.* Hydrogen Sulfide Protects from Colitis and Restores Intestinal Microbiota Biofilm and Mucus Production. *Inflamm Bowel Dis* <background-color:#FFCC66;bvertical-align:super;>21</background-color:#FFCC66;bvertical-align:super;>, 1006–1017 (2015).
7. Hu, L.-F. *et al.* Neuroprotective effects of hydrogen sulfide on Parkinson's disease rat models. *Aging Cell* <background-color:#FFCC66;bvertical-align:super;>9</background-color:#FFCC66;bvertical-align:super;>, 135–146 (2010).
8. Stevens, L. J., Burgess, J. R., Stochelski, M. A. & Kuczek, T. Amounts of Artificial Food Dyes and Added Sugars in Foods and Sweets Commonly Consumed by Children. *Clin Pediatr (Phila)* <background-color:#FFCC66;bvertical-align:super;>54</background-color:#FFCC66;bvertical-align:super;>, 309–321 (2015).
9. Zou, L. *et al.* Bacterial metabolism rescues the inhibition of intestinal drug absorption by food and drug additives. *Proc Natl Acad Sci USA* <background-color:#FFCC66;bvertical-align:super;>117</background-color:#FFCC66;bvertical-align:super;>, 16009–16018 (2020).

10. He, Z. *et al.* Food colorants metabolized by commensal bacteria promote colitis in mice with dysregulated expression of interleukin-23. *Cell Metabolism* <background-color:#FFCC66;bvertical-align:super;>33</background-color:#FFCC66;bvertical-align:super;>, 1358–1371.e5 (2021).
11. Blachier, F. *et al.* Luminal sulfide and large intestine mucosa: friend or foe? *Amino Acids* <background-color:#FFCC66;bvertical-align:super;>39</background-color:#FFCC66;bvertical-align:super;>, 335–347 (2010).
12. Pereira, F. C. & Berry, D. Microbial nutrient niches in the gut. *Environ Microbiol* <background-color:#FFCC66;bvertical-align:super;>19</background-color:#FFCC66;bvertical-align:super;>, 1366–1378 (2017).
13. Ryan, A. Azoreductases in drug metabolism. *British Journal of Pharmacology* <background-color:#FFCC66;bvertical-align:super;>174</background-color:#FFCC66;bvertical-align:super;>, 2161–2173 (2017).
14. van der Zee, F. P. *et al.* The contribution of biotic and abiotic processes during azo dye reduction in anaerobic sludge. *Water Research* <background-color:#FFCC66;bvertical-align:super;>37</background-color:#FFCC66;bvertical-align:super;>, 3098–3109 (2003).
15. Costa, M. C., Mota, F. S. B., Santos, A. B. D., Mendonça, G. L. F. & Nascimento, R. F. do. Effect of dye structure and redox mediators on anaerobic azo and anthraquinone dye reduction. *Quím. Nova* <background-color:#FFCC66;bvertical-align:super;>35</background-color:#FFCC66;bvertical-align:super;>, 482–486 (2012).
16. Zee, F. P. van der, Bouwman, R. H. M., Strik, D. P. B. T. B., Lettinga, G. & Field, J. A. Application of redox mediators to accelerate the transformation of reactive azo dyes in anaerobic bioreactors. *Biotechnology and Bioengineering* <background-color:#FFCC66;bvertical-align:super;>75</background-color:#FFCC66;bvertical-align:super;>, 691–701 (2001).
17. Awano, N., Wada, M., Mori, H., Nakamori, S. & Takagi, H. Identification and Functional Analysis of Escherichia coli Cysteine Desulfhydrases. *Appl. Environ. Microbiol.* <background-color:#FFCC66;bvertical-align:super;>71</background-color:#FFCC66;bvertical-align:super;>, 4149–4152 (2005).
18. Lobel, L., Cao, Y. G., Fenn, K., Glickman, J. N. & Garrett, W. S. Diet posttranslationally modifies the mouse gut microbial proteome to modulate renal function. *Science* <background-color:#FFCC66;bvertical-align:super;>369</background-color:#FFCC66;bvertical-align:super;>, 1518–1524 (2020).
19. Loddeke, M. *et al.* Anaerobic Cysteine Degradation and Potential Metabolic Coordination in Salmonella enterica and Escherichia coli. *J Bacteriol* <background-color:#FFCC66;bvertical-align:super;>199</background-color:#FFCC66;bvertical-align:super;>, (2017).
20. Nayfach, S., Fischbach, M. A. & Pollard, K. S. MetaQuery: a web server for rapid annotation and quantitative analysis of specific genes in the human gut microbiome. *Bioinformatics* <background-color:#FFCC66;bvertical-align:super;>31</background-color:#FFCC66;bvertical-align:super;>, 3368–3370 (2015).

21. Bastie, C. C. *et al.* Dietary Cholecalciferol and Calcium Levels in a Western-Style Defined Rodent Diet Alter Energy Metabolism and Inflammatory Responses in Mice. *The Journal of Nutrition* <background-color:#FFCC66;bvertical-align:super;>142</background-color:#FFCC66;bvertical-align:super;>, 859–865 (2012).
22. Miller, R. A. *et al.* Methionine-deficient diet extends mouse lifespan, slows immune and lens aging, alters glucose, T4, IGF-I and insulin levels, and increases hepatocyte MIF levels and stress resistance: Methionine restriction slows mouse aging, R. A. Miller et al. *Aging Cell* <background-color:#FFCC66;bvertical-align:super;>4</background-color:#FFCC66;bvertical-align:super;>, 119–125 (2005).
23. Reese, A. T. *et al.* Antibiotic-induced changes in the microbiota disrupt redox dynamics in the gut. *eLife* <background-color:#FFCC66;bvertical-align:super;>7</background-color:#FFCC66;bvertical-align:super;>, e35987 (2018).
24. Shatalin, K. *et al.* Inhibitors of bacterial H2S biogenesis targeting antibiotic resistance and tolerance. *Science* <background-color:#FFCC66;bvertical-align:super;>372</background-color:#FFCC66;bvertical-align:super;>, 1169–1175 (2021).
25. Kondo, K. *et al.* H2S Protects Against Pressure Overload–Induced Heart Failure via Upregulation of Endothelial Nitric Oxide Synthase. *Circulation* <background-color:#FFCC66;bvertical-align:super;>127</background-color:#FFCC66;bvertical-align:super;>, 1116–1127 (2013).
26. Yang, G. *et al.* H2S as a Physiologic Vasorelaxant: Hypertension in Mice with Deletion of Cystathionine -Lyase. *Science* <background-color:#FFCC66;bvertical-align:super;>322</background-color:#FFCC66;bvertical-align:super;>, 587–590 (2008).
27. Wolfe, R. S. Techniques for Cultivating Methanogens. in *Methods in Enzymology* vol. 494 1–22 (Elsevier, 2011).
28. A. Webster, T., J. Sismaet, H., J. Chan, I. -ping & D. Goluch, E. Electrochemically monitoring the antibiotic susceptibility of Pseudomonas aeruginosa biofilms. *Analyst* <background-color:#FFCC66;bvertical-align:super;>140</background-color:#FFCC66;bvertical-align:super;>, 7195–7201 (2015).
29. R Core Team. R: A language and environment for statistical computing. *R Foundation for Statistical Computing, Vienna, Austria.* (2020).
30. Wickham, H. *ggplot2: Elegant Graphics for Data Analysis*. (Springer-Verlag, 2016).
31. Cline, J. D. Spectrophotometric determination of hydrogen sulfide in natural waters. *Limnol. Oceanogr.* <background-color:#FFCC66;bvertical-align:super;>14</background-color:#FFCC66;bvertical-align:super;>, 454–458 (1969).
32. Strocchi, A., Furne, J. K. & Levitt, M. D. A modification of the methylene blue method to measure bacterial production in feces. *Journal of Microbiological Methods* <background-color:#FFCC66;bvertical-align:super;>15</background-color:#FFCC66;bvertical-align:super;>, 75–82 (1992).

33. Benson, D. A. *et al.* GenBank. *Nucleic Acids Research* <background-color:#FFCC66;bvertical-align:super;>41</background-color:#FFCC66;bvertical-align:super;>, D36–D42 (2013).
34. Kanehisa, M. & Goto, S. KEGG: Kyoto Encyclopedia of Genes and Genomes. *Nucleic Acids Research* <background-color:#FFCC66;bvertical-align:super;>28</background-color:#FFCC66;bvertical-align:super;>, 27–30 (2000).
35. Huerta-Cepas, J. *et al.* eggNOG 4.5: a hierarchical orthology framework with improved functional annotations for eukaryotic, prokaryotic and viral sequences. *Nucleic Acids Research* <background-color:#FFCC66;bvertical-align:super;>44</background-color:#FFCC66;bvertical-align:super;>, D286–D293 (2016).
36. Edgar, R. C. Search and clustering orders of magnitude faster than BLAST. *Bioinformatics* <background-color:#FFCC66;bvertical-align:super;>26</background-color:#FFCC66;bvertical-align:super;>, 2460–2461 (2010).
37. Edgar, R. C. MUSCLE: multiple sequence alignment with high accuracy and high throughput. *Nucleic Acids Res.* <background-color:#FFCC66;bvertical-align:super;>32</background-color:#FFCC66;bvertical-align:super;>, 1792–1797 (2004).
38. Eddy, S. R. Accelerated Profile HMM Searches. *PLOS Computational Biology* <background-color:#FFCC66;bvertical-align:super;>7</background-color:#FFCC66;bvertical-align:super;>, e1002195 (2011).
39. Pasolli, E. *et al.* Accessible, curated metagenomic data through ExperimentHub. *Nat Methods* <background-color:#FFCC66;bvertical-align:super;>14</background-color:#FFCC66;bvertical-align:super;>, 1023–1024 (2017).
40. Segata, N. *et al.* Metagenomic microbial community profiling using unique clade-specific marker genes. *Nat Methods* <background-color:#FFCC66;bvertical-align:super;>9</background-color:#FFCC66;bvertical-align:super;>, 811–814 (2012).
41. F, M. *et al.* The EMBL-EBI search and sequence analysis tools APIs in 2019. *Nucleic Acids Res* <background-color:#FFCC66;bvertical-align:super;>47</background-color:#FFCC66;bvertical-align:super;>, W636–W641 (2019).
42. Trifinopoulos, J., Nguyen, L.-T., von Haeseler, A. & Minh, B. Q. W-IQ-TREE: a fast online phylogenetic tool for maximum likelihood analysis. *Nucleic Acids Research* <background-color:#FFCC66;bvertical-align:super;>44</background-color:#FFCC66;bvertical-align:super;>, W232–W235 (2016).
43. Letunic, I. & Bork, P. Interactive Tree Of Life (iTOL) v5: an online tool for phylogenetic tree display and annotation. *Nucleic Acids Research* (2021) doi:10.1093/nar/gkab301.

Declarations

Data Availability Statement

The authors declare that the data supporting the findings of this study are available within the paper and its supplementary information files.

Acknowledgments

The authors thank Ali Ryan (Northumbria University) for sharing his knowledge of azoreductase enzymes, and the laboratories of Steven Almo and Tyler Grove (Albert Einstein College of Medicine) for experimental and intellectual support in related work. Libusha Kelly was supported by a United States Department of Defense Cancer Research Program Career Development Award (CA171019). Reese Hitchings was supported by the Albert Einstein College of Medicine PhD in Clinical Investigation training grant TL1 TR001072. Leonard Augenlicht was supported by the National Cancer Institute Department of Cancer Prevention Nutrition grants 1R01CA214625 and 1R01CA229216. Support was also received by the Albert Einstein Cancer Center core support grant P30CA013330.

Author Contributions

SW, RH, LK, and LA drafted the manuscript. SW performed *E. coli* experiments, metagenomic analysis, and mouse fecal sulfide determination. RH performed abiotic and fecal slurry experiments, as well as mass spectrometry. KP performed all mouse experimentation and maintained the mouse colony. LA guided mouse experiments and diet formulation. TY performed cyclic voltammetry of azo compounds. EG guided electrochemistry experiments. MM and ZC assisted with fecal slurry experiments. SK assisted with metagenomic analysis. All authors edited manuscript and contributed intellectually.

Competing Interest Declaration

The authors declare no competing interests.

Methods

Abiotic Azoreduction Assay

The capacity for H_2S to abiotically reduce azo compounds common in foods and drugs was investigated in a sterile, anoxic phosphate buffer medium. Serum bottles were prepared by sparging with ultrapure (99.9%) N_2 flowed over a heated copper catalyst to remove impurities[27]. Bottles were stoppered and capped under positive N_2 pressure and autoclaved 3 times on successive days. The medium contained final concentrations of 3 mM sulfide delivered as Na_2S, 50 mM $NaPO_4$ buffer (pH 6.3), 25 μM FMN, and 500 μM azo-compound. Bottles were incubated at 37°C with shaking and sampled using sterile anoxic technique. To halt the reaction, 5 mM ZnAc was pre-dispensed into tubes so the sample was immediately submerged in ZnAc solution. Samples were vortexed for 1min and stored at -80°C. For mass spectrometry analysis, samples were centrifuged at 14,000xg for 5 min, and the supernatants were analyzed. Redox

potentials of the experimental azo compounds were calculating using a multipotentiostat (CHI 1040C A2728)[28]. Three cycles of cyclic voltammetry scans were collected using a rod-shaped glassy carbon working electrode, carbon counter electrodes and silver/silver-chloride (Ag/AgCl) paste reference electrode connected to the multipotentiostat at various scan rate settings to observe the reduction potentials of test molecules.

LC-MS of Azo-compounds and Azoreduction Products

Liquid Chromatography

Chromatography was performed on an Agilent 1200-series HPLC coupled to a 6130 Single-Quadrupole Mass Spectrometer (Agilent Technologies, Santa Clara, CA). Liquid chromatography was performed using an Agilent Poroshell 120 EC-C18, 21x50mm, 2.7nm. The mobile phases used were 2mM NH_4Ac in H_2O +0.1% formic acid (mobile phase A), and 2mM NH_4Ac in MeOH +0.1% formic acid (mobile phase B). The column was maintained at 25°C, while the autosampler was maintained at 4°C. Elution schemes for each drug and metabolite are reported in Supplementary Table 3.

Mass Spectrometry

Ions were analyzed using single ion monitoring in either positive or negative mode, using *m/z* for each metabolite reported in Supplementary Table 3. Drying gas was set at 12 L/min, nebulizer pressure at 35 psig, drying gas at 350°C, fragmentor at 70V, and capillary voltage at 3000V. Identity of all compounds was verified by retention time and m/z of authentic, commercially available standards, except for the azoreduction products of Yellow 6 and Congo red, which were unavailable commercially. For these compounds, we identified species with predicted m/z values that increased in intensity at the same relative rate at which the parent compound decreased in our abiotic experiment.

Statistical analysis

Statistical analysis was performed in R (version 3.6.3,[29]) and plotted with the package ggplot2 (ggplot2 3.3.3,[30]) or in Graphpad Prism 8.

Hydrogen sulfide analysis

Hydrogen sulfide was quantified using a modified methylene blue detection assay[31,32]. For liquid microbial culture, 30 µL sample was collected using strict anoxic technique and immediately dispensed

into 157 µL ZnAc (28 g/L). This was diluted with 1.26 mL H_2O, followed by the addition of 113 µL Cline's Reagent (N,N-dimethyl-p-phenylenediamine and $FeCl_3 \cdot 6H_2O$ in 50% HCl). The reaction was incubated at room temperature for 20 minutes to allow complete color development. Samples were centrifuged to remove particulates and 100 µL supernatant was transferred into Corning Costar half area 96-well flat bottom plates (Corning Inc., Corning, NY). Hydrogen sulfide concentrations were quantified using UV-vis detection at a wavelength of 670 nm on a BioTek Synergy H4 plate reader (BioTek Instruments, Winooski, VT) and quantified using Gen5 version 1.11 software.

E. coli pure cultures

E. coli K-12 W3100 (Carolina Biological, Burlington, NC) was grown in anoxic LB supplemented with 25 mM FMN and 30 mM succinate for all experiments. To minimize headspace and encourage hydrogen sulfide partitioning to the liquid fraction, 8 mL cultures were grown in 10 mL serum bottles under an N_2 atmosphere, sealed with butyl rubber stoppers and aluminum crimps, and incubated at 37°C. All conditions were established in triplicate. Samples were extracted from sealed bottles by syringe using sterile anaerobic technique.

Live E. coli

Sulfide azoreduction and enzymatic azoreductase activity were compared in growth phase *E. coli* cultures. Cysteine served as a readily metabolized thiol source. The scheme of culture conditions can be seen in Supplemental Table 4. Experimental conditions received 2 mM L-cysteine and Red 40 amended at 3.0 mM, 0.5 mM, or 0.25 mM. To quantify the maximum potential sulfide generated from cysteine, cultures were spiked with 2 mM cysteine but no Red 40 ("No Red 40"). Three control conditions were established. The first, "Enzymatic Control", monitored *E. coli* azoreduction and hydrogen sulfide production in bottles receiving 0.25 mM Red 40 but no supplemental amino acid. The second set of controls received 2 mM L-serine as a nonsulfur cysteine analog, to account for any growth advantage effect of excess amino acid ("AA Control"). These control cultures served to quantify baseline enzymatic azoreductase activity, while the cysteine amended cultures would in theory azoreduce Red 40 via both enzymatic azoreductase activity and sulfide azoreduction. A sterile, uninoculated media control containing media and 0.25 mM Red 40 was also monitored for abiotic activity in the media itself ("Background"). Each condition was monitored for Red 40 loss and hydrogen sulfide generation.

Heat-inactivated E. coli

The *E. coli* experiment was replicated using heat-killed *E. coli* to eliminate all enzymatic activity, including azoreductases. Cultures of *E. coli* were incubated with the addition of either 2 mM cysteine or serine for

18 hours and then heat-inactivated by autoclave. Autoclaving the sealed bottles allowed for cell death and enzyme denaturing without breaching the headspace, maintaining both dissolved and gas phase H_2S. Following 1 hour of cooling and equilibration, H_2S concentration was measured and bottles then immediately amended with 3.0, 0.5, or 0.25 mM Red 40. An additional 25 mM FMN was supplemented to replace any portion lost to heat-inactivation. H_2S and Red 40 concentrations were monitored for 6 hours.

Biological Culture Red 40 Analysis

Red 40 concentrations were quantified using UV-vis detection at a wavelength of 489 nm in Corning Costar half area 96-well flat bottom plates (Corning Inc., Corning, NY) on a BioTek Synergy H4 plate reader (BioTek Instruments, Winooski, VT) and quantified using Gen5 version 1.11 software. Timepoints were diluted 1:1 with water and quantification was performed by linear regression of known standards.

Fecal Microcosm Azoreduction

The ability of a complex fecal microbiome community to azoreduce Red 40 both with and without dietary and endogenous sulfur sources was determined in fecal microcosms. Microcosms were established as 1% feces (w/v) in defined chemical medium as described in detail below. A freshly voided fecal sample was collected from a volunteer with no known health conditions who had not used antibiotics within 6 months. This study was approved by the Einstein Institutional Review Board (IRB#2013-2895). Defined chemical medium was prepared under anaerobic conditions by boiling and sparging with ultrapure (99.9%) N_2 scrubbed as before, with the following final concentrations: 9 mM Na_2HPO_4, 31 mM NaH_2PO_4, 24 mM $NaHCO_3$, 0.3 mM $(NH_4)_2SO_4$, 14.4 mM NaCl, 25 µM riboflavin, 20.5 µM $CaCl_2$ $2H_2O$, 50.5 µM $MnCl_2$ $4H_2O$, 98.4 µM $MgCl_2$ $6H_2O$, 4.2 µM $CoCl_2$ $6H_2O$, Widdel trace elements andvitamins[41], 0.77 µM (0.5 µg/mL) hemin, 100 µM DTT and 20 mM glucose. 8 mL cultures were grown in 10 mL serum bottles under an N_2 atmosphere, sealed with butyl rubber stoppers and aluminum crimps, and incubated at 37°C. All conditions were established in triplicate. Base media before addition of feces was added to serum bottles as sterile controls. Fecal sample was homogenized in 10mL media with sterile glass beads by vigorous shaking and added anoxically to the base media to a final concentration of 1% feces (w/v). This unamended fecal slurry was placed in serum bottles to serve as *heat-killed controls* and immediately autoclaved before incubating at 37°C for 12 hours. This process was repeated twice before supplementation with Red 40. For the *Mucin, BSA,* and *Formaldehyde controls,* fecal slurry was supplemented with 0.4% (w/v) type III porcine gastric mucin, 1% Bovine Serum Albumin, and 4% paraformaldehyde, respectively, before aliquoting into serum bottles. *Cysteine* and *Serine* conditions were supplemented with 10 mM of the appropriate amino acid; *Background* was not supplemented to show baseline hydrogen sulfide production. Once all culture bottles had been assembled, they were supplemented with Red 40 to a final concentration of 500 µM (Supplementary Table 5).

Cysteine Degrading Gene Analysis

Nine genes encoding enzymes with characterized cysteine-degrading activity[17–19,24] were evaluated in human gut metagenomic samples and in commensal gut microbes: CBS (K01697), CSE (K01758), CysK (K01738), CysM (K12339), CyuA (COG3681), MalY (K14155), MetC (K01760), SseA (K01011) and TnaA (K01667).

Metaquery Analysis for Mean Copy Number Per Cell in Human Gut Microbiomes

The KEGG or COG orthologue of each gene was searched within the 2,522 annotated metagenomic samples in the Metaquery[20] database. For each gene, the copy number per cell in each metagenomic sample was averaged and reported in Figure 3c.

Gut Commensal Genomic Analysis of Cysteine Degrading Genes

To identify the presence or absence of the nine cysteine degrading genes, databases of homologous sequences for each gene were constructed and searched against 24,758 NCBI bacterial genomes (Genbank, April 2021[33]).

The reference protein database for each gene was derived from the sequence from the organism in which it was originally characterized[17]. A KEGG web server[34] BLASTP search of these genes, limited to bacteria, provided 500 closely related orthologues ($\leq 1e^{-75}$) from other species.

CyuA (formerly YhaM[19]) is not catalogued in the KEGG database. Reference sequences were instead retrieved from COG3681 in the EggNOG database (EggNOG 4.5.1[35]). To reduce the number of sequences to approximately 500 to facilitate alignment, sequences were clustered at 77% identity with usearch cluster_fast (Usearch 8,[36]) and centroids were used in the reference database.

Sequences in each gene's reference protein database were aligned using MUSCLE with default parameters (MUSCLE 3.8.1551,[37]) and alignments were used to construct Hidden Markov Models using hmmbuild with default parameters (hmmer 3.3.2,[38]). The 9 hmms were searched against the 24,758 bacterial genomes using hmmsearch with a stringent cutoff of $1e^{-10}$. One hit in a genome indicated

presence of the gene in a particular genome; multiple hits were ignored (Supplementary Table 6). We then narrowed the output to a subset of bacteria commonly found in the human gut microbiome. To identify relevant gut microbes we procured 8,548 metagenomic samples of patients from 51 studies using the R package curatedMetagenomicData[39]. For each of these samples, we downloaded a list of relative abundances of 6,832 taxa annotated using the MetaPhlAn2[40] software for each of these studies. We computed the mean relative abundance across studies for each taxa and selected organisms with ≥0.05% mean relative abundance and manual curation. Finally, different strains within the same species with the same pattern of cysteine degrading genes were clustered. By doing so we were able to observe intra-species diversity of cysteine degrading genes while eliminating duplicates.

A phylogenetic tree of the stool organisms of interest was constructed using 16S rRNA nucleotide sequences associated with each genome assembly in NCBI. 16S sequences were aligned using MUSCLE with default parameters via the EMBL-EBI search and analysis tool [41]. A maximum likelihood tree was constructed using the IQ-TREE web server with 1000 ultrafast bootstrap analysis, an automatically selected substitution model and otherwise default parameters[42] and visualized in iTOL[43].

Mouse Housing and Diet

To assess the influence of varying dietary cysteine concentrations on fecal H_2S, three separate cohorts of 10 3-week old male weanling C57BL/6J mice were randomly assigned to each of three diets varying in cysteine (Control, 0 Cys, and High Cys; Supplementary Table 2) (N = 30, 10/diet). 2-5 mice per cage were co-housed with ad-libitum access to their assigned diet and water. We then followed this experiment with a crossover experiment adding Red 40 to the control diet as a potential redox partner for H_2S. For the crossover experiment, two cohorts of 6 3-week old male weanling C57BL/6J mice were assigned to either the Control diet or Red 40 diet (Supplementary Table 2) (N=12, 6/diet). Each cohort of 6 mice was split into two cages, 3 mice per cage.

Mouse Fecal Sulfide Sampling

Fecal sulfide was measured twice per week in all mice consuming Control, 0 Cys, or High Cys diets. Mice co-housed in each condition were placed in a clean collection tray and allowed to freely defecate for one hour, at which point 7-9 random fecal pellets were collected and separately placed in pre-weighed tubes containing 157 µL of 28 g/L Zinc Acetate. These samples were vortexed and stored at 4°C until analysis by Cline assay. During the crossover experiment fecal sulfide was measured more frequently, 2-5 times per week. Each mouse was placed in a separate collection tray to ensure one pellet per mouse, and, following defecation, pellets were collected and stored as above.

Figures

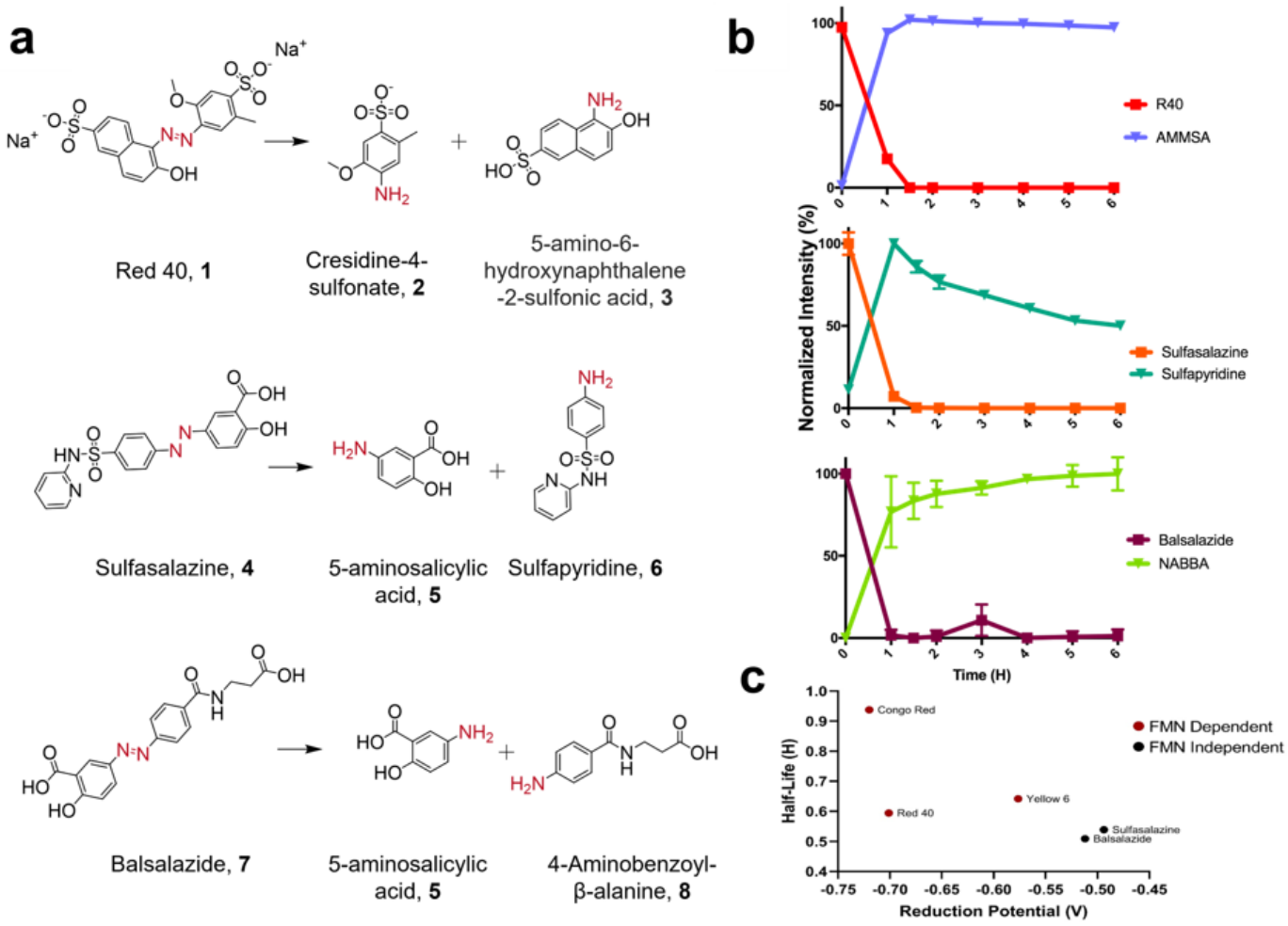

Figure 1

Sulfide reduces diverse azo compounds. a, Structures of three common gut-relevant azo compounds and azoreduction products. b) Normalized MS intensities of parent compound (squares) and azoreduced product (triangles) over time when incubated with sulfide in a sterile, anoxic environment. c) Relationship between reduction potential of azo bond measured by cyclic voltammetry and half-life of azo compounds determined as in b.

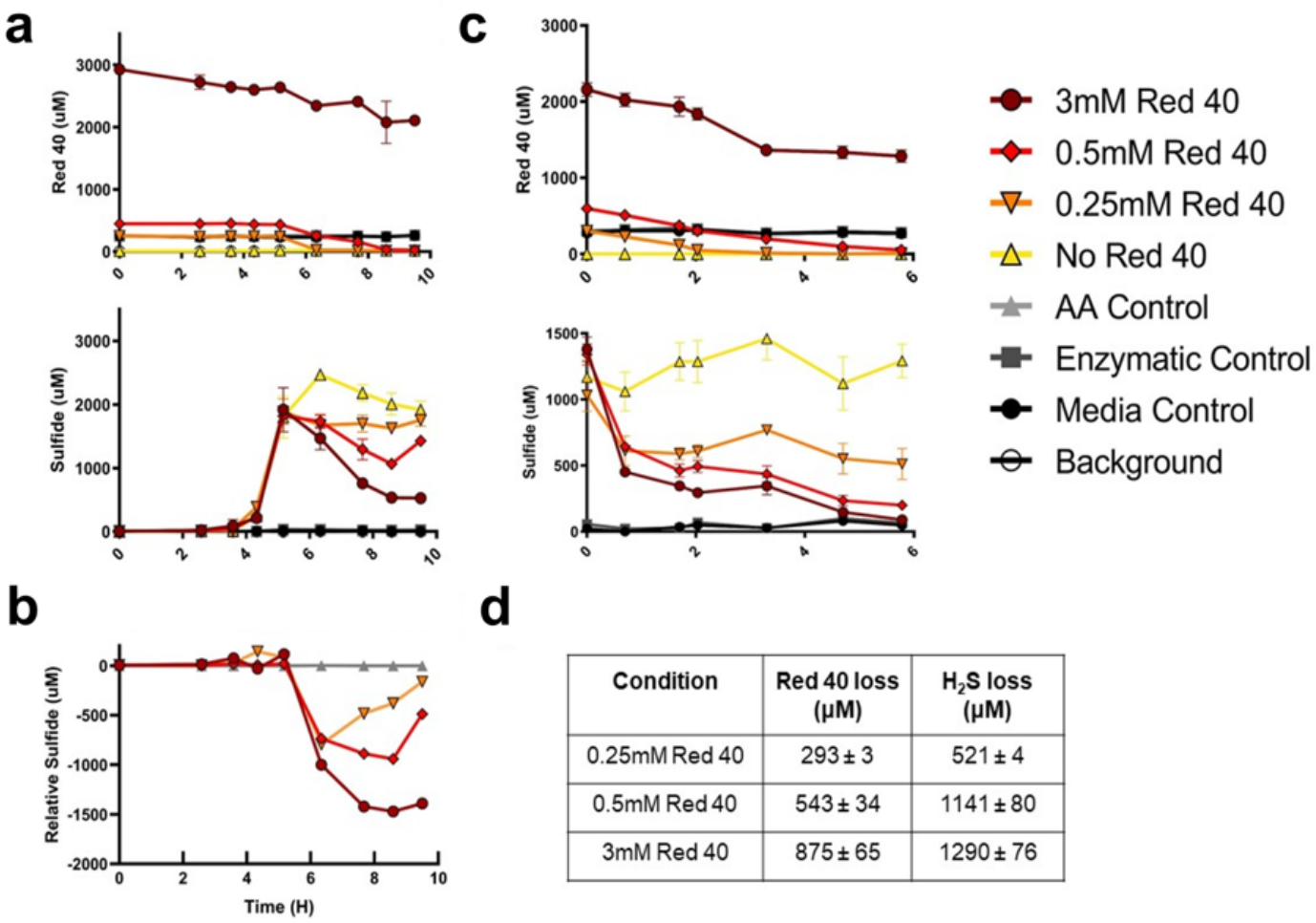

Condition	Red 40 loss (µM)	H_2S loss (µM)
0.25mM Red 40	293 ± 3	521 ± 4
0.5mM Red 40	543 ± 34	1141 ± 80
3mM Red 40	875 ± 65	1290 ± 76

Figure 2

Anaerobic E. coli azoreduces via sulfide production. a, Anoxic E. coli cultures fed 2mM cysteine were supplemented with increasing concentrations of Red 40. Red 40 (top) and sulfide (bottom) were quantified spectrophotometrically. b, Sulfide per Red 40 condition as in A, relative to “AA control”. c, E. coli cultures prepared as in A were allowed to accumulate sulfide overnight before autoclaving and supplementation with Red 40. d, Red 40 and sulfide loss (mean ± sd) from c. Sulfide and Red 40 decrease at an approximate 2:1 ratio, matching predicted stoichiometry.

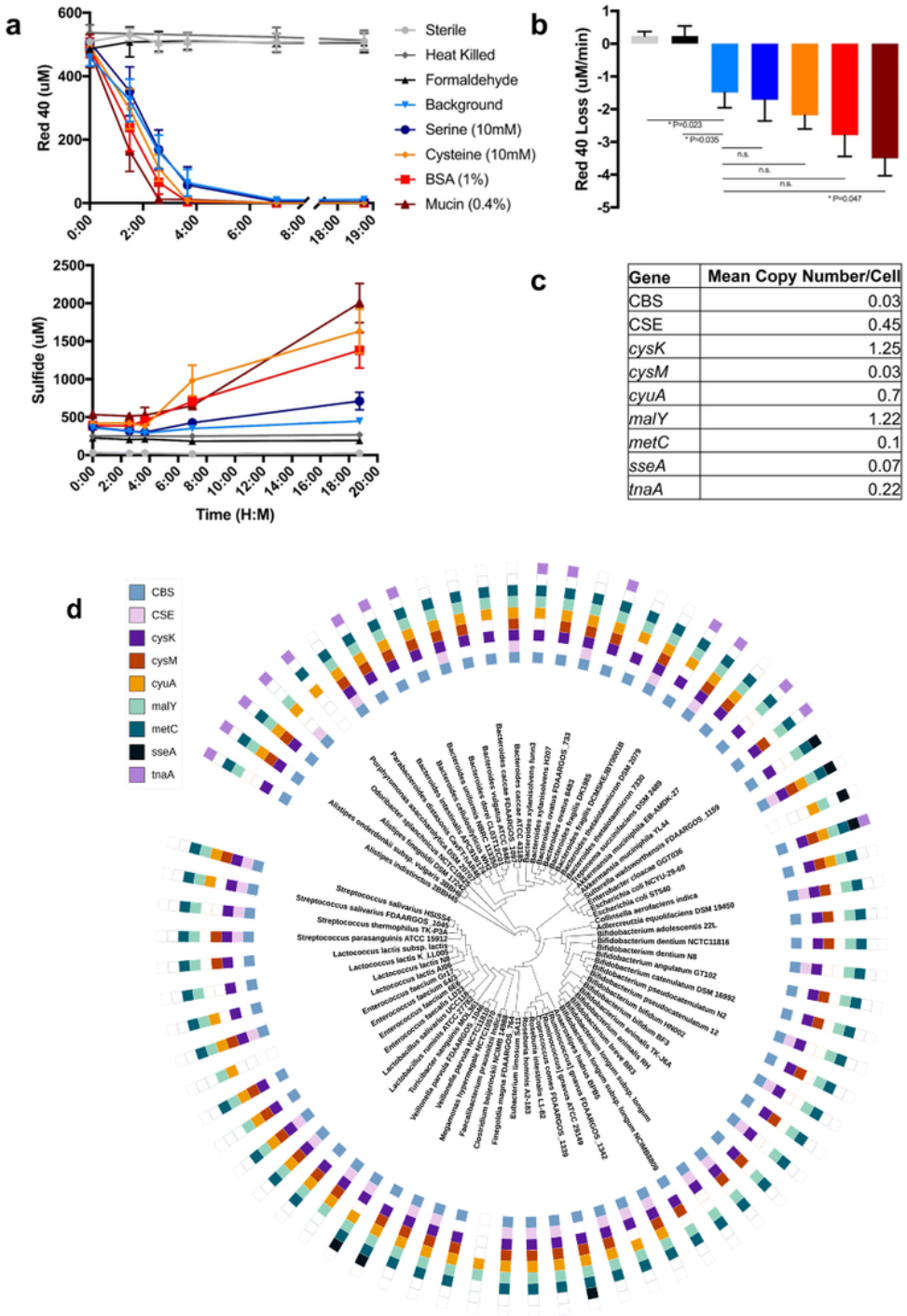

Gene	Mean Copy Number/Cell
CBS	0.03
CSE	0.45
cysK	1.25
cysM	0.03
cyuA	0.7
malY	1.22
metC	0.1
sseA	0.07
tnaA	0.22

Figure 3

Human Fecal Microbiomes Reduce Red 40 in Proportion to Available Thiol Sources. a, Red 40 (top) and sulfide (bottom) concentrations over time in a healthy human fecal community reconstituted in minimal anaerobic media and supplemented with different thiol sources. Warm colors indicate conditions that received thiol sources, cool colors have only thiol sources present in the fecal sample. b, Initial rate of azoreduction for each condition. Conditions azoreduce at different rates (ANOVA, p=0.0004), Mucin

azoreduces faster than background (Dunnett's multiple comparisons test, p=0.047). c, Mean copy number of bacterial cysteine degrading genes across 2k+ human gut microbiome samples identified by Metaquery20. d, Sulfidogenic cysteine degrading genes identified in the complete genomes of common human gut microbes.

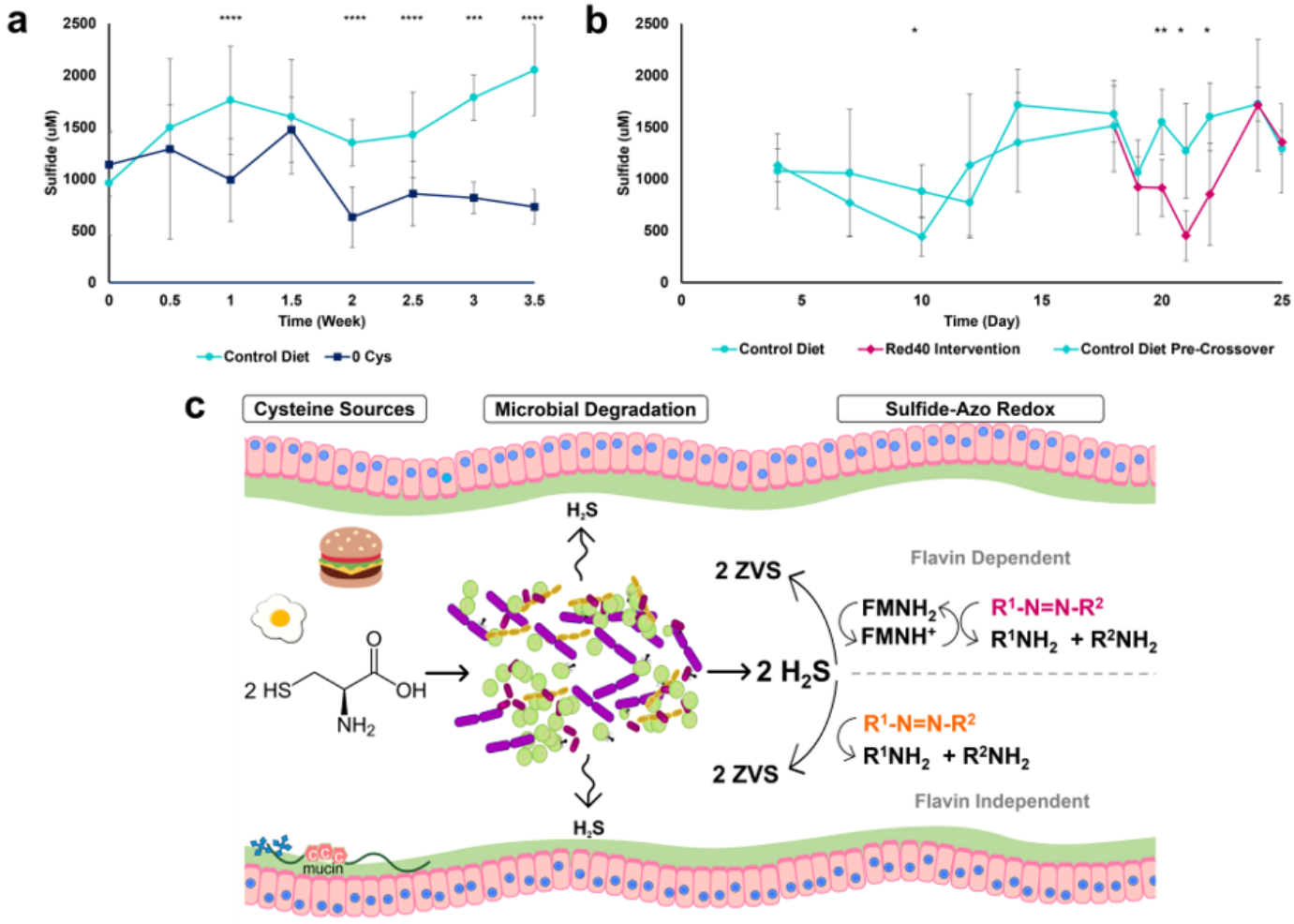

Figure 4

Diet Alters Fecal Sulfide in Mice. a, Fecal sulfide measured from representative mice fed diets containing 0 g/kg cysteine (dark blue) or standard 4 g/kg cysteine (light blue). Mice on a diet with no cysteine had less fecal sulfide than mice consuming standard cysteine after two weeks (Wilcoxon rank-sum, p<0.001,). b, Fecal sulfide measured from mice consuming a standard 4 g/kg cysteine. At day 18, one cohort (indicated in red) was administered Red 40 and a transient decrease in sulfide was observed (Wilcoxon rank-sum, p<0.01, day 20, p<0.05 day 21,22). c, Proposed mechanism of sulfide-azo redox in the gut. Cysteine, consumed in food and present in endogenous compounds, is metabolized by the human gut microbiota. Dissimilatory degradation releases H2S to the lumen where it can interact with the host, microbes, and chemicals. Here we provide evidence of redox chemistry with xenobiotic food and drugs, in which two molecules of hydrogen sulfide donate four electrons to an azo bond, releasing two corresponding amine products and oxidizing H2S to zero valent sulfur.

Supplementary Files

This is a list of supplementary files associated with this preprint. Click to download.

- SupplementaryTables.xlsx
- SupplementaryFigures.docx